Protein Engineering

DOI: 10.1002/ange.200600382

Engineering Proteins with Novel Mechanical Properties by Recombination of Protein Fragments**

*Deepak Sharma, Yi Cao, and Hongbin Li**

The mechanical properties of proteins are crucial in living cells as proteins serve as basic units in cells to constantly sense, generate, and bear mechanical forces.[1,2] Outside the cell, nature exploits the mechanical features of proteins and produces a variety of materials with superb mechanical properties (e.g. spider dragline silk[3,4]) which often outperform man-made materials. Studies of the mechanics of proteins are not only important in understanding fundamental biophysical principles underlying various biological processes,[5] but they also underscore the great potential in engineering protein-based advanced materials and using proteins as building blocks for the bottom-up construction of functional nanomechanical devices.[6]

Despite the great significance of mechanical proteins, the investigation of the mechanical design of these proteins at the single-molecule level was not possible until the development of single-molecule force spectroscopy techniques a few years ago.[7–11] Since then, single-molecule atomic force microscopy (AFM) has become the workhorse in the field of protein nanomechanics.[5,12–15] Initial single-molecule AFM studies focused on naturally occurring mechanical proteins that are placed under stretching force under physiological conditions, such as the immunoglobulin (Ig) domains of the giant muscle protein titin and the fibronectin type III domains from fibronectin and tenascin.[7,10,11,16–19] Recently, non-mechanical proteins have also been studied by single-molecule force spectroscopy in the search for mechanically stable protein folds and to expand the toolbox of mechanical proteins.[20–25] With the increasing understanding of the relationship between protein structure and protein mechanical stability, scientists have attempted to engineer or modify the mechanical properties of proteins. Such efforts are limited to site-directed mutagenesis.[19,26–28] With the advent of nanobiotechnology, it is desired to engineer novel multifunctional mechanical proteins that combine desired mechanical properties with other functional properties, such as enzymatic activity. Site-directed mutagenesis may not suffice for such challenges. Here, we demonstrate the feasibility and the first attempt towards engineering novel mechanical proteins through DNA-shuffling-based recombination.

Recombination is an important mechanism for proteins to acquire novel functions. Recombination offers the advantage of combining beneficial mutations from multiple parents into a single offspring and has been exploited extensively by nature during evolution in improving protein traits such as enzymatic activity. This method has also been used extensively in the directed-evolution of proteins in the laboratory and has become one of the most important strategies in engineering proteins with novel functions.[29,30] Recombination is based on DNA-shuffling of proteins sharing high sequence homology and identity. Recent developments have extended this method to proteins that are distantly related and share low sequence homology.[31,32] Here, as a proof of principle, we demonstrate the feasibility of using this powerful method to engineer proteins with novel mechanical stability. This will serve as the first step towards engineering multifunctional proteins in which mechanical stability is combined with desired additional functionality.

We used the 27th and 32nd immunoglobulin domains (I27 and I32, following the nomenclature by Labeit[33]) from human cardiac titin as the parent model proteins to construct

[*] Dr. D. Sharma, Y. Cao, Prof. Dr. H. Li
Department of Chemistry
The University of British Columbia
2036 Main Mall
Vancouver BC, V6T1Z1 (Canada)
Fax: (+1) 604-822-2847
E-mail: Hongbin@chem.ubc.ca

[**] This work was supported by the Natural Sciences and Engineering Research Council of Canada, Canada Research Chairs program, Canada Foundation for Innovation, and Peter Wall Institute for Advanced Studies and by start-up fund from the University of British Columbia. Y.C. was supported in part by the Laird Fellowship.

Supporting information for this article is available on the WWW under http://www.angewandte.org or from the author.

hybrid proteins by recombining different fragments from the two parents. I27 and I32 are good model systems for mechanical proteins and have been studied extensively by single-molecule AFM.[7,11,16,27] It was shown that I27 unfolds at a force of ≈200 pN while I32 is mechanically more stable and unfolds at a force of ≈300 pN.[11,16] The big difference in their mechanical stability may have interesting ramifications for the mechanical properties of hybrid recombinant proteins.

Extensive single-molecule atomic force microscopy studies,[11,26–28,34,35] in conjunction with steered molecular dynamics simulations,[36–39] revealed the critical importance of the A′ and G β strands (referred to as the A′G patch) to the mechanical stability of the I27 domain. When I27 is stretched from its N and C termini, a shear force is applied to the hydrogen-bonding network in the A′G patch, which forms the force-bearing parts of I27 and constitutes the strongest mechanical resistance to unfolding. This shear topology of the hydrogen-bonding network seems to be a common feature among stable mechanical proteins,[11,22,25,28] and suggests that mechanical stability may be a rather local phenomenon. Hence, it seems possible to modulate the mechanical properties of I27-like proteins by shuffling the A′G patch among I27 homologous proteins. Here, we show that, by interchanging the force-bearing A′ and G strands or the presumably non-force-bearing C, D, and E strands between I27 and I32, we can successfully generate mechanically stable, hybrid proteins. To the best of our knowledge, this is the first successful recombination approach to impart novel mechanical properties to proteins.

I27 and I32 share a high sequence homology (identity 42%, similarity 57%, according to the program CLUSTALW, Figure 1A). Although the three-dimensional structure of I32 has not yet been determined, co-evolution and similar functional properties suggest that I32 shares high structural homology with I27. Structural homology modeling using the web-based package Swiss-Model by First Approach Mode (URL: http://swissmodel.expasy.org/) showed that I32 adopts a β-sandwich structure (Figure 1B, green) that is similar to that of I27[40] (Figure 1B, yellow). The hybrid proteins were designed such that they contain both A′ and G β strands from the same parent (Figure 1B) to have minimal disruption of interactions between these two strands, which are presumably important for the mechanical stability. Crossover points were selected at the loops to minimize the interference of the packing of the β-sandwich structure. Using this approach, we shuffled the fragments of both proteins (see the Experimental Section) and constructed four hybrids, I27-A′G-I32, I32-A′G-I27, I27-CDE-I32 and I32-CDE-I27, where the force-bearing A′ and G strands (for the first two hybrids) or non-force-bearing C, D, and E strands (for the latter two hybrids) are interchanged between I27 and I32 (Figure 1B). I27-A′G-I32 stands for a hybrid protein in which A′ and G strands come from I32, while the rest come from parent protein I27. I27-CDE-I32 stands for a hybrid protein in which the C, D, and E strands come from I32, and the remaining come from I27. The other two hybrid proteins are named accordingly (Figure 1B).

To efficiently screen and test the mechanical properties of the hybrid proteins, we constructed a polyprotein containing the recombined hybrid Ig domain flanked by four tandem

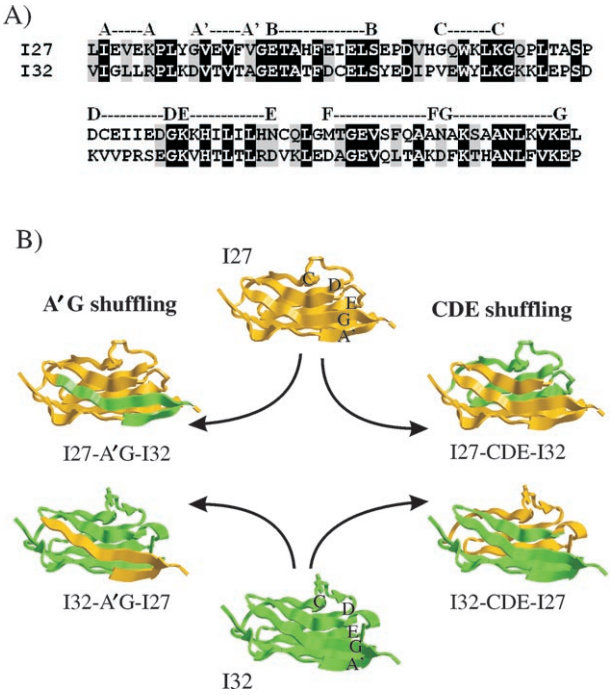

Figure 1. Engineering novel mechanical proteins by recombination of protein fragments from I27 and I32. A) Sequence alignment between parent proteins I27 and I32 shows high sequence homology (57% similarity) between the two proteins. Gray shading indicates homology, inverse text (white on black background) indicates identity. B) Designed hybrid Ig domains. Middle column shows the three-dimensional structures of I27 (Protein Database code: 1TIT,[40] yellow) and I32 (green). I32 structure was obtained by homology modeling (see text). By interchanging the A′ and G β strands between I27 and I32, we designed hybrid proteins I27-A′G-I32 and I32-A′G-I27 (left column). Interchanging the C, D, and E β strands between I27 and I32 resulted in hybrid proteins I27-CDE-I32 and I32-CDE-I27 (right column). In the hybrid proteins, the fragments coming from the wild-type I27 are shown in yellow, while those from wild-type I32 are shown in green.

GB1 domains at the N and C termini (Figure 2A), as described in the Experimental Section. The well-characterized GB1 protein[25] serves as an internal caliper for identifying single-molecule stretching events[41] as well as pinning down the mechanical signature of the hybrid Ig domains. A 1-μL droplet of the purified polyprotein solution (≈100 ng) was deposited on a clean glass cover slip, and the polyprotein was stretched between an AFM tip and glass substrate in phosphate-buffered saline (PBS).

Stretching $(GB1)_4$-I27-A′G-I32-$(GB1)_4$ results in force–extension curves having a characteristic sawtooth pattern like those in Figure 2B. Individual force peaks correspond to the mechanical unraveling of the individual protein domains being stretched.[7,11] The last force peak corresponds to the stretching of the fully unfolded polypeptide and its subsequent detachment from the surface of the glass substrate or AFM tip. Fits according to the worm-like chain model (WLC)[42] of polymer elasticity are shown as dotted lines (Figure 2B).

If we observe five or more unfolding events of GB1 in one force–extension curve, we are certain that one I27-A′G-I32

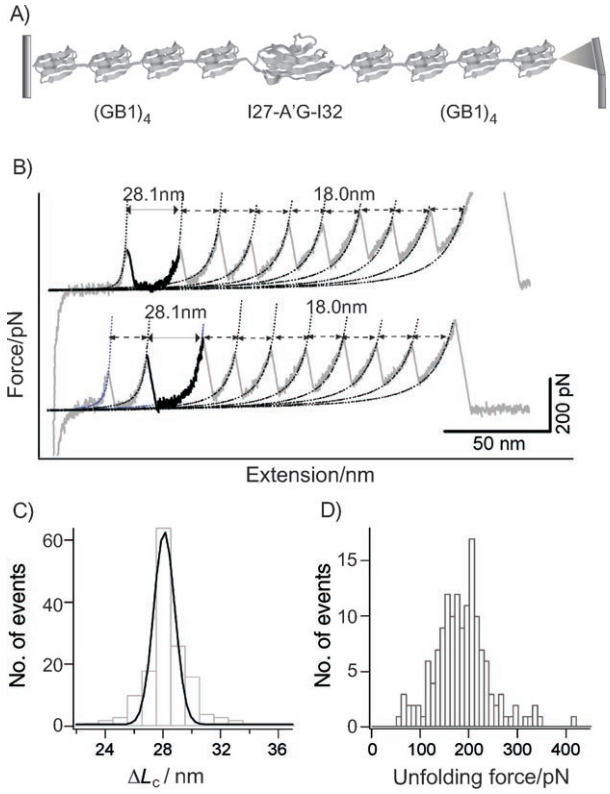

Figure 2. Mechanical properties for the hybrid I27-A′G-I32 protein. A) Representation of the chimera polyprotein $(GB1)_4$-I27-A′G-I32-$(GB1)_4$ being stretched between the AFM tip and glass substrate. B) Two representative force–extension curves for stretching chimera polyprotein $(GB1)_4$-I27-A′G-I32-$(GB1)_4$. Dotted lines correspond to WLC fits to the force–extension data. Contour length increments ΔL_c between consecutive unfolding events are indicated between WLC fits. The force peaks corresponding to the mechanical unfolding events of GB1 are in gray, while the unfolding event with $\Delta L_c \approx 28$ nm corresponds to the unfolding of the folded hybrid I27-A′G-I32 protein (in black). C) Histogram of ΔL_c for the unfolding of the hybrid I27-A′G-I32, which corresponds to the events in black in Figure 2B. A Gaussian fit to the histogram shows an average ΔL_c of 28.1 ± 0.7 nm, confirming that I27-A′G-I32 acquires a folded structure similar to that of the wild-type I27. D) Unfolding force frequency histogram for the recombined I27-A′G-I32 shows an average unfolding force of $\approx 178 \pm 44$ pN ($n = 149$) at a pulling speed of 400 nm s^{-1}.

domain has been stretched, since I27-A′G-I32 is flanked by $(GB1)_4$ on both termini. The unfolding events of GB1 can be readily recognized[25] by their characteristic contour length increment (ΔL_c) of ≈ 18 nm. Similarly, the unfolding of I27-A′G-I32 can be identified by its own characteristic ΔL_c value. The contour length increment is an intrinsic structural parameter of a folded protein and can be used to infer structural information about a protein.[34,43] I27-A′G-I32 comprises 89 amino acids (aa) and is 32 nm long when it is fully stretched (89aa × 0.36 nm per aa = 32 nm), the same as wild-type (wt-) I27 and wt-I32. If the hybrid protein folds into a stable three-dimensional structure similar to that of I27 and I32, the distance between the N and C termini of the hybrid Ig domain in the folded state will be also similar to that of I27 and I32, which is ≈ 4.3 nm.[40] The complete mechanical unfolding of the hybrid protein will result in $\Delta L_c \approx 28$ nm (32 nm − 4.3 nm = 27.7 nm), similar to that of I27 and I32 (Table 1). Therefore, the mechanical unfolding of the folded hybrid Ig domain will manifest itself in the force–extension curve as an unfolding event with $\Delta L_c \approx 28$ nm. Indeed, in the

Table 1: Mechanical properties of the recombined hybrid proteins.

	Unfolding force (±SD) [pN]	Contour length increment (±SD) [nm]
wt-I27[a]	204(±26)	28.1 ± 0.2
wt-I32[b]	298(±24)	28
I27-A′G-I32	178(±44)	28.1(±0.7)
I27-CDE-I32	212(±35)	27.9(±0.6)
I32-A′G-I27	229(±87)	28.0(±0.6)
I32-CDE-I27	147(±40)	28.1(±0.6)

[a] Reference [11]. [b] Reference [16].

force–extension recordings of $(GB1)_4$-I27-A′G-I32-$(GB1)_4$ having more than five GB1 unfolding events ($\Delta L_c \approx 18$ nm), we always observe one unfolding event with contour length increment of ≈ 28 nm, in good agreement with the polyprotein we constructed. A histogram of ΔL_c for these events shows an average of 28.1 nm for ΔL_c (Figure 2C). Therefore, these events correspond to the mechanical unfolding of I27-A′G-I32, indicating that I27-A′G-I32 is folded and mechanically resistant. An unfolding force histogram shows an average unfolding force of ≈ 178 pN ($n = 149$) (Figure 2D).

Similarly, we observed unfolding events with $\Delta L_c \approx 28$ nm (Figure 3A, C, and E) in force–extension curves of all other three recombined hybrid Ig domains. These events correspond to the mechanical unfolding of the designed hybrid Ig

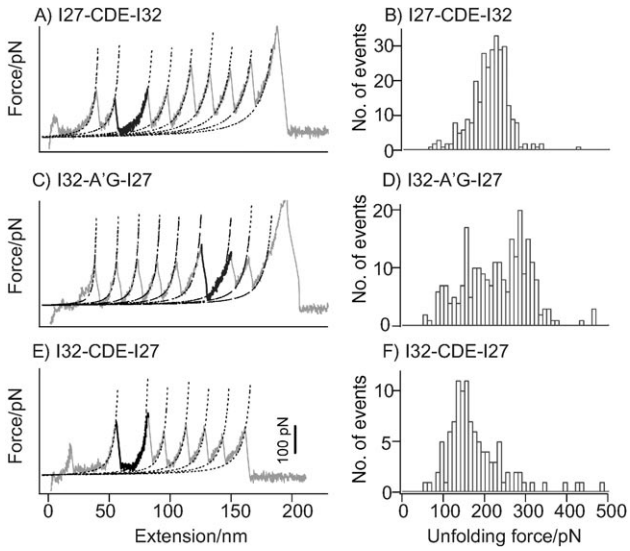

Figure 3. Typical force–extension curves and unfolding force histograms for the recombined hybrid Ig domains: A), B) for I27-CDE-I32, C), D) for I32-A′G-I27, and E), F) for I32-CDE-I27. In A), C), and E) the unfolding events of hybrid Ig domains are in black, while the unfolding of GB1 domains are in gray. Approximations by the WLC model are shown as dotted lines. The average unfolding force is 212 ± 35 pN ($n = 293$) for I27-CDE-I32, 229 ± 87 pN ($n = 255$) for I32-A′G-I27, and 147 ± 40 pN ($n = 107$) for I32-CDE-I27.

domains. The unfolding force histograms of the three hybrid proteins are shown in Figure 3B, D, and F. These results confirmed that all the three recombined hybrid Ig domains are folded and mechanically resistant. The fact that the contour length increment (see the Supporting Information) is similar to that of the wt-I27 and wt-I32 indicates that these three hybrid Ig domains acquired three-dimensional structures that are similar to those of the wild-type domains. The mechanical properties of the four hybrid Ig domains are summarized in Table 1. It is evident that the four hybrid Ig domains show novel and diverse mechanical stability, with unfolding forces ranging from $\approx$150 pN to 230 pN, which is different from that of the parent wt-I27 and wt-I32. The distribution of the unfolding forces for the hybrids (I27-A′G-I32, I27-CDE-I32, and I32-CDE-I27) is slightly broader than that of wt-I27 and wt-I32. This broadening may have resulted from the fact that the loading rate for the stretching of hybrid Ig domains varies due to the unfolding of the fingerprint GB1 domains in the construct. However, the unfolding force distribution of I32-A′G-I27 is significantly broader, suggesting its uniqueness to I32-A′G-I27.

To ensure that such a broad distribution for I32-A′G-I27 is not an artifact caused by the AFM methodology we used, we have constructed a polyprotein chimera [GB1-(I32-A′G-I27)]$_4$ (see the Supporting Information) and carried out single-molecule AFM measurements. The use of GB1 in this polyprotein chimera allows us to identify the mechanical unfolding events of I32-A′G-I27 unambiguously. (The force–extension curves of this polyprotein chimera, as well as the unfolding force histogram of I32-A′G-I27, are shown in the Supporting Information.) The unfolding force histogram of I32-A′G-I27 shows a broad distribution, which is in close agreement with the result shown in Figure 3D. This result corroborates that the broad distribution of unfolding forces is indeed an intrinsic property of the recombined I32-A′G-I27 domain. However, its molecular origin remains unknown. Much more in-depth experimental and simulation efforts will be required to find a molecular-level explanation for such a broad distribution. These efforts will involve the illustration of the three-dimensional structure of the protein, detailed molecular dynamics simulation of the mechanical unfolding process, and site-directed mutagenesis.

Our conclusion that all four engineered hybrid Ig domains are folded is further corroborated by structural evaluation using far-UV circular dichroism (CD) spectroscopy. Figure 4 shows the far-UV CD spectra of the four isolated hybrid Ig domains, which were expressed as individual monomers (see the Experimental Section). The CD spectra of the four engineered Ig domains are characteristic of a predominantly β-sheet secondary structure and are similar to that of the parent protein I27 reported previously.[44] In addition, CD measurements (see the Supporting Information) on the polyprotein chimera [GB1-(I32-A′G-I27)]$_4$ showed that the flanking of recombined Ig domain with GB1 does not change the secondary structure of Ig domains. These results confirm that the engineered hybrid domains are indeed folded into structures similar to those of the wild-type parent proteins and that the novel mechanical properties of the engineered proteins indeed result from recombination.

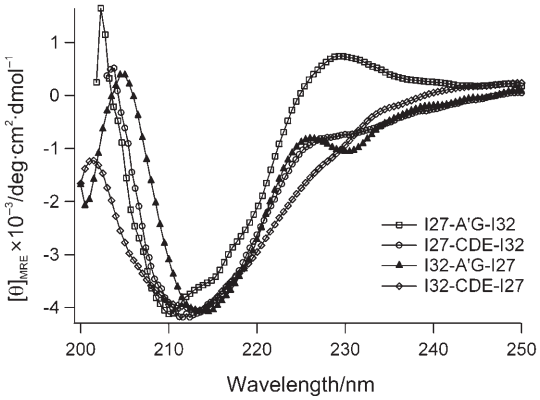

Figure 4. Far-UV CD spectra for the recombined hybrid Ig domains. Spectra were obtained using a cuvette (path length 0.2 cm) at a scan rate of 20 nm min^{-1}. Each curve was obtained by averaging three scans. CD spectra of all four designed hybrid proteins are typical of β-sheet proteins.

Previous studies have identified that the A′G patch is the key element that imparts the mechanical resistance to I27.[26,36–38,45] Owing to the high structural homology between I27 and I32, we expect that the same rule also applies to I32. The backbone hydrogen bonds linking A′ and G β strands are identified to be the main origin of the mechanical strength. If A′G is the sole region important for mechanical stability, one would expect that I27-A′G-I32 and I32-CDE-I27 will be mechanically as stable as the wt-I32, as the force-bearing A′G patch of wt-I32 is preserved in both hybrid Ig domains. Similarly, the mechanical stability of I32-A′G-I27 and I27-CDE-I32 would be similar to that of the wt-I27. However, both I27-A′G-I32 and I32-CDE-I27 unfold at much lower forces than wt-I32 (178 pN and 147 pN versus the expected 300 pN for wt-I32), while I32-A′G-I27 is mechanically stronger than wt-I27 (229 pN versus the expected 200 pN for wt-I27). These results clearly suggest that the A′G patch may not be the only structural region responsible for the mechanical stability of Ig domains. Additional interactions and structures that are coupled to the A′G patch may also play important roles in determining the mechanical stability of Ig domains. For example, the hydrophobic packing of the two β sheets may also be one important factor in determining the mechanical stability of Ig domains. This finding resembles those found in recombination-based directed evolution of enzymes: although the active site of an enzyme is composed of only a few key residues, structures distant from the active site as well as those adjacent ones can have a profound effect on the outcome of the enzymatic activities.[30,46]

These "unexpected" results reveal richer structural information and details that one can utilize to further tailor the mechanical and other functional properties of proteins through protein-engineering tools. This perspective offers great promise for engineering proteins with much more diverse mechanical stability and functionality from two parent proteins with well-defined mechanical stability.

In summary, we have demonstrated the first successful attempt to engineer novel mechanically stable proteins by shuffling protein fragments among two homologous parent

proteins. We showed that by recombination the four designed hybrid Ig domains based on I27 and I32 fold into three-dimensional structures that are similar to the wild-type parent proteins. In addition the hybrid Ig domains are mechanically stable. The methodology demonstrated here is an exciting new application of the powerful recombination technique in the field of protein mechanics and opens a new way to tailor proteins' mechanical properties. This study also serves as the first step towards engineering mechanical proteins with multiple functionalities, which will find useful applications in bionanotechnology by serving as building blocks for nanomechanical devices. Future work will involve combining high-accuracy homology modeling and experimental recombination work to extend the current methodology to a series of homologous Ig domains with the aim of constructing a combinatorial mechanical protein library.

Experimental Section

wt-I27 and I32, carrying a 5′ *BamH*I and a 3′ *Bgl*II and *Kpn*I restriction site, were amplified from an Ig8-GFP plasmid[21] encoding I27 to I34 of human cardiac titin and GFP (a generous gift from Dr. Matthias Rief) using standard PCR techniques and subcloned into pUC19 vector to generate pUC19-I27 and pUC19-I32, respectively.

Plasmid containing the designed hybrid I27-A′G-I32 gene was generated using the megaprimer method.[47] DNA that encodes residues 15–78 of I27 was amplified using wt-I27 as a template. Forward and reverse primers for this PCR encode the A′ strand (residues 11–14) and the G strand (residues 79–88) of I32, respectively. Both primers are flanked with sequences of wt-I27 (one to four residues) at their 5′ and 3′ ends. Amplified product was gel-purified and subsequently used as megaprimer to generate pUC19-I27-A′G-I32 using pUC19-I27 as the PCR template. Similarly, pUC19-I32-A′G-I27 was constructed.

pUC19-I27-CDE-I32 and pUC19-I32-CDE-I27 were generated as follows: Restrictions sites ApaI and AgeI were introduced into I27 and I32 after residues 28 and 67, respectively, by site-directed mutagenesis, leading to plasmids pUC19-I27(a-a) and pUC19-I32 (a-a). Insert encoding residues 29–66 of I27, which corresponds to the CDE region along with its adjacent loops, was obtained after digestion of pUC19-I27(a-a) with ApaI and AgeI. The insert was then ligated into the pUC19-I32(a-a) vector, which was linearized by *Apa*I and *Age*I restriction enzymes, to produce pUC19-I32-CDE-I27. pUC19-I27-CDE-I32 was obtained similarly. All sequences were confirmed by DNA sequencing.

Protein expression was carried out in pQE80L expression vector. $(GB1)_4$ polyprotein gene was obtained by a procedure similar to that described previously for $(GB1)_8$.[25] For expression of I27-A′G-I32, pUC19-I27-A′G-I32 was digested with restriction enzymes *BamH*I and *Kpn*I. The insert released was subcloned into vector pQE80L-$(GB1)_4$, which was digested with enzymes *Bgl*II and *Kpn*I, to generate pQE80L-$(GB1)_4$-I27-A′G-I32. $(GB1)_4$ flanked with *BamH*I and *Kpn*I was further subcloned into pQE80L-$(GB1)_4$-I27-A′G-I32 digested with *Bgl*II and *Kpn*I. The other three hybrid protein expression vectors were constructed in a similar fashion. The expression vector contained an N-terminal six-residue histidine tag to facilitate purification of expressed proteins. Two additional Cys residues were included at the 3′ end of the gene. The polyprotein was expressed in DH5α strain and purified using Ni-NTA (NTA = nitrilotriacetic acid; *N*,*N*-bis(carboxymethyl)glycine) affinity chromatography. The protein samples were kept in PBS buffer containing 200 mM imidazole with 5 mM 1,4-dithiothreitol to prevent air-oxidation of cysteine residues at 4 °C.

For circular dichroism (CD) studies, individual hybrid Ig domains were directly subcloned into the pQE80L expression vector using restriction sites BamHI and KpnI. Proteins were expressed in DH5α strain and purified using Ni-NTA affinity chromatography. Proteins were eluted in PBS buffer containing 200 mM imidazole. Eluted proteins were extensively dialyzed against 0.5 × PBS before CD measurements.

Single-molecule AFM experiments were carried out on a custom-built atomic force microscope, which was constructed as described previously.[48] The spring constant of each individual cantilever (Si_3N_4 cantilevers from Vecco, with a typical spring constant of 40 pN nm^{-1}) was calibrated in solution using the equipartition theorem before and after each experiment.[49,50] All the force–extension measurements were carried out in PBS buffer. A 1-μL droplet of the polyprotein solution ($\approx$100 ng) was placed on a clean glass cover slip covered by PBS buffer. It was allowed to absorb for 5 min and was then stretched between the AFM tip and glass substrate at a pulling speed of 400 nm s^{-1}.

CD spectra in the far-UV range were recorded on a Jasco-J810 spectropolarimeter flushed with nitrogen gas. The spectra were recorded in a cuvette with a path length of 0.2 cm at a scan rate of 20 nm min^{-1}. For each protein sample an average of three scans was reported. Data was corrected for buffer contributions. Results are expressed as mean residue ellipticity (θ_{MRE}), calculated according to Equation (1), where θ_{obs} is the observed ellipticity (in deg), d is path length (in cm), C is concentration of protein samples (M), and n is total number of amino acids in the protein.

$$\theta_{MRE} = (100\,\theta_{obs})/[d\,C\,(n-1)] \quad (1)$$

Received: January 29, 2006
Revised: May 12, 2006
Published online: July 20, 2006

Keywords: protein engineering · protein structures · scanning probe microscopy · single-molecule studies

[1] G. Bao, S. Suresh, *Nat. Mater.* **2003**, *2*, 715.
[2] A. S. Tatham, P. R. Shewry, *Trends Biochem. Sci.* **2000**, *25*, 567.
[3] N. Becker, E. Oroudjev, S. Mutz, J. P. Cleveland, P. K. Hansma, C. Y. Hayashi, D. E. Makarov, H. G. Hansma, *Nat. Mater.* **2003**, *2*, 278.
[4] J. C. van Hest, D. A. Tirrell, *Chem. Commun.* **2001**, 1897.
[5] T. E. Fisher, A. F. Oberhauser, M. Carrion-Vazquez, P. E. Marszalek, J. M. Fernandez, *Trends Biochem. Sci.* **1999**, *24*, 379.
[6] D. S. Goodsell, *Bionanotechnology*, Wiley-Liss, Hoboken, **2004**.
[7] M. Rief, M. Gautel, F. Oesterhelt, J. M. Fernandez, H. E. Gaub, *Science* **1997**, *276*, 1109.
[8] M. S. Kellermayer, S. B. Smith, H. L. Granzier, C. Bustamante, *Science* **1997**, *276*, 1112.
[9] L. Tskhovrebova, J. Trinick, J. A. Sleep, R. M. Simmons, *Nature* **1997**, *387*, 308.
[10] A. F. Oberhauser, P. E. Marszalek, H. P. Erickson, J. M. Fernandez, *Nature* **1998**, *393*, 181.
[11] M. Carrion-Vazquez, A. F. Oberhauser, S. B. Fowler, P. E. Marszalek, S. E. Broedel, J. Clarke, J. M. Fernandez, *Proc. Natl. Acad. Sci. USA* **1999**, *96*, 3694.
[12] M. Carrion-Vazquez, A. F. Oberhauser, T. E. Fisher, P. E. Marszalek, H. B. Li, J. M. Fernandez, *Prog. Biophys. Mol. Biol.* **2000**, *74*, 63.
[13] R. B. Best, D. J. Brockwell, J. L. Toca-Herrera, A. W. Blake, D. A. Smith, S. E. Radford, J. Clarke, *Anal. Chim. Acta* **2003**, *479*, 87.
[14] X. Zhuang, M. Rief, *Curr. Opin. Struct. Biol.* **2003**, *13*, 88.
[15] B. Samori, G. Zuccheri, P. Baschieri, *ChemPhysChem* **2005**, *6*, 29.

[16] H. Li, W. A. Linke, A. F. Oberhauser, M. Carrion-Vazquez, J. G. Kerkvliet, H. Lu, P. E. Marszalek, J. M. Fernandez, *Nature* **2002**, *418*, 998.
[17] A. F. Oberhauser, C. Badilla-Fernandez, M. Carrion-Vazquez, J. M. Fernandez, *J. Mol. Biol.* **2002**, *319*, 433.
[18] S. P. Ng, R. W. Rounsevell, A. Steward, C. D. Geierhaas, P. M. Williams, E. Paci, J. Clarke, *J. Mol. Biol.* **2005**, *350*, 776.
[19] D. J. Brockwell, G. S. Beddard, J. Clarkson, R. C. Zinober, A. W. Blake, J. Trinick, P. D. Olmsted, D. A. Smith, S. E. Radford, *Biophys. J.* **2002**, *83*, 458.
[20] G. Yang, C. Cecconi, W. A. Baase, I. R. Vetter, W. A. Breyer, J. A. Haack, B. W. Matthews, F. W. Dahlquist, C. Bustamante, *Proc. Natl. Acad. Sci. USA* **2000**, *97*, 139.
[21] H. Dietz, M. Rief, *Proc. Natl. Acad. Sci. USA* **2004**, *101*, 16192.
[22] D. J. Brockwell, G. S. Beddard, E. Paci, D. K. West, P. D. Olmsted, D. A. Smith, S. E. Radford, *Biophys. J.* **2005**, *89*, 506.
[23] R. B. Best, B. Li, A. Steward, V. Daggett, J. Clarke, *Biophys. J.* **2001**, *81*, 2344.
[24] C. Cecconi, E. A. Shank, C. Bustamante, S. Marqusee, *Science* **2005**, *309*, 2057.
[25] Y. Cao, C. Lam, M. Wang, H. Li, *Angew. Chem.* **2006**, *45*, 658; *Angew. Chem. Int. Ed.* **2006**, *45*, 642.
[26] H. Li, M. Carrion-Vazquez, A. F. Oberhauser, P. E. Marszalek, J. M. Fernandez, *Nat. Struct. Biol.* **2000**, *7*, 1117.
[27] P. M. Williams, S. B. Fowler, R. B. Best, J. L. Toca-Herrera, K. A. Scott, A. Steward, J. Clarke, *Nature* **2003**, *422*, 446.
[28] H. Li, J. M. Fernandez, *J. Mol. Biol.* **2003**, *334*, 75.
[29] J. D. Bloom, M. M. Meyer, P. Meinhold, C. R. Otey, D. MacMillan, F. H. Arnold, *Curr. Opin. Struct. Biol.* **2005**, *15*, 447.
[30] C. A. Voigt, C. Martinez, Z. G. Wang, S. L. Mayo, F. H. Arnold, *Nat. Struct. Biol.* **2002**, *9*, 553.
[31] J. A. Bittker, B. V. Le, J. M. Liu, D. R. Liu, *Proc. Natl. Acad. Sci. USA* **2004**, *101*, 7011.
[32] K. E. Griswold, Y. Kawarasaki, N. Ghoneim, S. J. Benkovic, B. L. Iverson, G. Georgiou, *Proc. Natl. Acad. Sci. USA* **2005**, *102*, 10082.
[33] S. Labeit, B. Kolmerer, *Science* **1995**, *270*, 293.
[34] M. Carrion-Vazquez, P. E. Marszalek, A. F. Oberhauser, J. M. Fernandez, *Proc. Natl. Acad. Sci. USA* **1999**, *96*, 11288.
[35] S. B. Fowler, R. B. Best, J. L. Toca Herrera, T. J. Rutherford, A. Steward, E. Paci, M. Karplus, J. Clarke, *J. Mol. Biol.* **2002**, *322*, 841.
[36] M. Gao, H. Lu, K. Schulten, *J. Muscle Res. Cell Motil.* **2002**, *23*, 513.
[37] H. Lu, B. Isralewitz, A. Krammer, V. Vogel, K. Schulten, *Biophys. J.* **1998**, *75*, 662.
[38] H. Lu, K. Schulten, *Biophys. J.* **2000**, *79*, 51.
[39] E. Paci, M. Karplus, *Proc. Natl. Acad. Sci. USA* **2000**, *97*, 6521.
[40] S. Improta, A. S. Politou, A. Pastore, *Structure* **1996**, *4*, 323.
[41] H. Li, A. F. Oberhauser, S. D. Redick, M. Carrion-Vazquez, H. P. Erickson, J. M. Fernandez, *Proc. Natl. Acad. Sci. USA* **2001**, *98*, 10682.
[42] J. F. Marko, E. D. Siggia, *Macromolecules* **1995**, *28*, 8759.
[43] H. Dietz, M. Rief, *Proc. Natl. Acad. Sci. USA* **2006**, *103*, 1244.
[44] A. S. Politou, D. J. Thomas, A. Pastore, *Biophys. J.* **1995**, *69*, 2601.
[45] D. K. West, D. J. Brockwell, P. D. Olmsted, S. E. Radford, E. Paci, *Biophys. J.* **2006**, *90*, 287.
[46] C. R. Otey, J. J. Silberg, C. A. Voigt, J. B. Endelman, G. Bandara, F. H. Arnold, *Chem. Biol.* **2004**, *11*, 309.
[47] G. Sarkar, S. S. Sommer, *Biotechniques* **1990**, *8*, 404.
[48] J. M. Fernandez, H. Li, *Science* **2004**, *303*, 1674.
[49] E. L. Florin, M. Rief, H. Lehmann, M. Ludwig, C. Dornmair, V. T. Moy, H. E. Gaub, *Biosens. Bioelectron.* **1995**, *10*, 895.
[50] J. L. Hutter, J. Bechhoefer, *Rev. Sci. Instrum.* **1993**, *64*, 3342.

